

Investigation of the broadband spatial correlation in a large reverberation chamber

Ingyu Chun^m ISVR, University of Southampton, Southampton, United Kingdom

Boaz Rafaely^m ISVR, University of Southampton, Southampton, United Kingdom

Phillip Joseph^m ISVR, University of Southampton, Southampton, United Kingdom

1. INTRODUCTION

The diffuse sound field model is widely used in the analysis of sound in reverberant rooms. In particular, the spatial correlation coefficient is an important measure for applications in which the diffuse field assumption is made, and its variation over several different directions is a measure of the diffuseness of reverberant field¹. For example, the spatial correlation coefficient can give an indication of the minimum permissible spacing of microphones necessary to obtain independent measurements of mean-square sound pressure for the determination of sound power levels in reverberation chambers^{2,3}. Another example is local active noise control in enclosed sound fields where performance depends upon the spatial correlation properties of the reverberant sound fields^{4,5}.

Many previous authors have studied theoretically and experimentally the spatial correlation coefficients for pure tone⁶ and narrowband diffuse fields^{7,8}. Recently, Rafaely⁹ has studied theoretically the spatial correlation in a diffuse field which is excited by a broadband random signal. The diffuse field spatial-temporal correlation function is generalized for stationary random signals with given power spectral density in his work.

This paper presents experimental verification of these theoretical results of broadband spatial correlation. This is achieved by measuring the spatial correlation coefficients in a large reverberant chamber excited by various broadband random signals and comparing the experimental results with the theoretical predictions.

2. Background theory

2.1 The definition of a diffuse sound field

The diffuse field can be defined as follows¹⁰: A diffuse sound field comprises a superposition of an infinite number of plane progressive waves, such that all directions of propagation are equally probable and plane waves constituting the field are statistically uncorrelated. This definition implies that the statistical quantity characterizing the diffuse sound field, such as the spatial correlation function, are spatially homogeneous and isotropic and the resultant acoustic intensity is zero everywhere¹¹. However, it is based on an idealized concept, that is, the state of the perfectly diffuse sound field cannot be usually met by any finite real space. Nevertheless, a reverberant sound field can be approximated by a diffuse field if it can be represented by a

sufficiently large number of plane waves. Therefore, broadband sound sources in a highly reverberant enclosure generate a quasi-diffuse field¹².

2.2 The Schroeder frequency

In a reverberant room, the average number of acoustic modes per unit frequency, that is the modal density, is approximately proportional to the square of frequency when room dimensions are large compared with a wavelength¹³. At very low frequencies, the modal density is very low, so that individual resonance peaks at the natural frequencies of the room are well separated in frequency compared to the half power bandwidth of the resonance peak of any single mode. As the frequency increases, the modal density increases, so that the individual resonance peaks are less distinct. There is a crossover frequency that indicates the transition from the region of well-separated resonance peaks to the region of many overlapping resonance peaks. However this crossover frequency is somewhat arbitrary. Schroeder suggested this crossover frequency, which is now known as the "Schroeder frequency". For airborne sound in a reverberant room, it is given by¹⁴

$$f_{sch} = \sqrt{\left(\frac{c_0^3 T_{60}}{4 \log_e 10 V} \right)} \approx 2000 \sqrt{\frac{T_{60}}{V}}$$

where c_0 is the speed of sound, T_{60} is the 60 dB reverberation time and V is the volume of the room in cubic meter. The expression for the Schroeder frequency can be simplified to the formula in Eq. using the factor 2000 for a moderate room temperature. On average, at least three resonance peaks lie within the half-power bandwidth of one resonance peak at frequencies above the Schroeder frequency.

3. Spatial correlation coefficient

3.1 Definition of the spatial correlation coefficient

The spatial-temporal correlation coefficient ρ between two position vectors \mathbf{x} and \mathbf{y} at times t_1 and t_2 respectively is defined as⁶

$$\rho(\mathbf{x}, t_1, \mathbf{y}, t_2) = \frac{E\{p(\mathbf{x}, t_1)p(\mathbf{y}, t_2)\}}{\sqrt{E\{p^2(\mathbf{x}, t_1)\}E\{p^2(\mathbf{y}, t_2)\}}}$$

where $E\{\}$ denotes the expectation operation, and p is the acoustic pressure. Note that the correlation coefficient ρ is between -1 and 1 .

We now assume that the acoustic pressure signals in space are stationary and ergodic with respect to time. The statistical properties are therefore unchanged under a shift in time, that is, the correlation coefficient is a function of time delay $\tau = |t_2 - t_1|$, and the ensemble average can be replaced by the time average. If the sound field is assumed to be perfectly diffuse, the acoustic pressure signals can be assumed to be stationary with respect to position, and so the statistical properties are unchanged under a shift in position, that is, the correlation coefficient is a function of the separation distance between two positions $r = |\mathbf{y} - \mathbf{x}|$. Moreover, they can be assumed to be ergodic with respect to position, that is, the ensemble statistics can be replaced by the spatial statistics⁷. Under the assumptions stated above, the spatial correlation coefficient averaged over time and space with zero time delay is therefore given by

$$\rho(r) = \lim_{N \rightarrow \infty} \lim_{T \rightarrow \infty} \frac{\sum_{n=1}^N \frac{1}{T} \int_0^T p(\mathbf{x}_n, t) p(\mathbf{y}_n, t) dt}{\sum_{n=1}^N \sqrt{\left\{ \frac{1}{T} \int_0^T p^2(\mathbf{x}_n, t) dt \right\} \left\{ \frac{1}{T} \int_0^T p^2(\mathbf{y}_n, t) dt \right\}}}$$

where T is the time duration of the acoustic pressure signals, the subscript n indicates the n th pair of randomly chosen discrete positions with constant distance $r = |\mathbf{y}_n - \mathbf{x}_n|$ between two positions, and N is the number of spatial averaging.

Equation is not adequate for the practical measurement of the spatial correlation coefficients in a reverberant field. The main reasons are as follows. First, since it is not possible to generate a perfectly diffuse field in any finite space, there would be some deviation from the assumptions used to derive Eq. . Second, N and T in Eq. are finite. Third, if the acoustic pressure signals are sampled by using an analogue-to-digital converter, the integral is replaced by a discrete summation. Therefore, the measured spatial correlation coefficient averaged over time and space with zero time delay is given by

$$\hat{\rho}(r) = \frac{\sum_{n=1}^N \sum_{m=0}^{M-1} \{ p(\mathbf{x}_n, m\Delta T) p(\mathbf{y}_n, m\Delta T) \}}{\sum_{n=1}^N \sqrt{\left\{ \sum_{m=0}^{M-1} p^2(\mathbf{x}_n, m\Delta T) \right\} \left\{ \sum_{m=0}^{M-1} p^2(\mathbf{y}_n, m\Delta T) \right\}}}$$

where M is the number of samples of the digital acoustic pressure signal in the time domain, m is an integer number and ΔT is the time resolution in seconds, which is equal to the inverse of the sample rate in hertz. The coefficient in Eq. provides an estimate of the coefficient in Eq. . Equation is the practical formula of the spatial correlation coefficient, and has been used in the experiment described in this paper.

3.2 Theoretical prediction of the spatial correlation coefficient

If a sound field is assumed to be perfectly diffuse, and stationary and ergodic with respect to time and space, the spatial correlation coefficient $\rho(r)$ with zero time delay can be written as⁹

$$\rho(r) = \frac{1}{\sigma^2} \int_{-\infty}^{\infty} S(f) \frac{\sin(kr)}{kr} df$$

where $S(f)$ is the power spectral density of the acoustic pressure signal exciting the infinite number of plane waves in a diffuse field, f is a frequency in hertz, k is the wave number

$$\left(k = \frac{2\pi f}{c_a} \right), \text{ and } \sigma^2 \text{ is the variance of the signal } \left(\sigma^2 = \int_{-\infty}^{\infty} S(f) df \right).$$

Equation is useful since the spatial correlation coefficient can be calculated if the power spectral density of the signal alone is known. It shows that the broadband spatial correlation coefficient equals to the integration of the pure tone spatial correlation coefficients⁶, i.e. a sinc function

$\left(\frac{\sin kr}{kr} \right)$, which is weighted by the normalized power spectral density of the signal over frequency. The experimental verification of Eq. is the main objective of this paper.

However, equation shows that the frequency range of the integral is from $-\infty$ to ∞ . In practice, the frequency range must be finite. If the analogue data acquired by the microphones are converted to digital data by an analogue-to-digital converter, the digital data are discrete and meaningful only below half the sample rate due to the mirror images produced in the sampling process. Therefore, equation can be approximated in practice by:

$$\hat{\rho}(r) = \frac{\sum_{l=0}^{L-1} G(l\Delta f) \frac{\sin(2\pi l\Delta f r/c_0)}{2\pi l\Delta f r/c_0}}{\sum_{l=0}^{L-1} G(l\Delta f)}$$

where the coefficient $\hat{\rho}(r)$ provides an estimate of the coefficient $\rho(r)$ in Eq. , $G(f)$ is the one-sided power spectral density of the signal, l is an integer number, L is the number of samples of the digital acoustic pressure signal up to half the sample rate in the frequency domain and Δf is the frequency resolution which is equal to half the sampling rate in hertz divided by L . Equation has been used to predict the broadband spatial correlation coefficients in this paper.

3.3 Validity of the generalized spatial correlation equation

Equation is based on the following assumptions: the sound field is perfectly diffuse; the sound field is stationary and ergodic with respect to time and space; the modal density is infinite over all frequencies. In practice, these assumptions cannot hold exactly. The theoretical prediction from Eq. or has two main sources of estimation errors originating from the validity of the two terms in the equation: the sinc function and the power spectral density.

First, the pure tone spatial correlation coefficient curve is not equal to the sinc function. The degree of deviation from the sinc function depends on the degree of diffuseness at the corresponding frequency. Second, at the low frequency range below the Schroeder frequency, modal density is low, that is, the individual resonance peaks are well separated and individually identified. Therefore, the room response at low frequencies and the response of the loudspeaker and microphone in an experiment can modify the power spectral density of the sound field. However, if the power spectral density measured in the reverberation chamber is substituted for Eq. instead of a theoretical power spectral density, the influence of this problem can be reduced.

4. EXPERIMENT

4.1 Experimental setup and procedure

The spatial correlation coefficients have been measured in a rectangular reverberation chamber whose volume is 348 m³. The Schroeder frequency of the reverberation chamber was calculated as 350Hz, which is a mean value of the Schroeder frequencies measured in one-third octave bands with centre frequencies from 100Hz to 1000Hz. The broadband random signals used in this experiment were generated by filtering normally distributed random signals through digital butterworth filters. The description of the test signals is shown in Table I. The first signal was chosen to investigate a broadband sound field of high modal overlap at frequencies above the Schroeder frequency, i.e. 350Hz, which was mixed with the sound field of low modal overlap at frequencies below the Schroeder frequency. The second signal was chosen to investigate the broadband sound field entirely below the Schroeder frequency, while the third signal was chosen to investigate the broadband sound field entirely above the Schroeder frequency.

The theoretical one-sided power spectral density of each signal is presented in Table II on the assumption that the power spectral density of the white noise signal S_w is a constant¹⁵. S_w will be removed by the normalizing process when the spatial correlation coefficient is calculated from Eq. or . Figure 1 shows the theoretical power spectral density of each test signal assuming S_w is unity.

Figure 2 shows a block diagram of the measurement system that consists of a sound generation system and a data acquisition system¹⁶. The accuracy of the magnitude of the output signal of the microphones is not significant in this experiment because the spatial correlation coefficients are calculated from normalized quantities. However, the phase difference between the two microphones is important because the correlation coefficient is based on the phase difference between the two signals. In this experiment, the Brüel & Kjær matched microphones type 4135 were chosen, with phase difference lower than 2.5° between 20Hz and 1kHz. The Brüel & Kjær sound intensity calibrator type 3541 was used to measure the phase difference. The gain of the power amplifier and measuring amplifiers was set to be sufficiently high to improve a signal-to-noise ratio, but adjusted not to exceed the analogue-to-digital convert (ADC) range. The generated digital signals were converted to analogue signal by the sound card mounted on PC with a sample rate of 16384Hz. The acquired analogue signals were sampled by the analogue-to-digital converter mounted on PC with a sample rate of 8192Hz. Because the roll off of the digital lowpass filter of each test signal was sufficiently fast at 1kHz, the cut-off frequency of both analogue lowpass filters was set for 1300Hz to avoid aliasing effects or mirror images without distorting the signals.

The loudspeaker was placed at the corner of the reverberation chamber. The measurement positions were at least one meter away from the walls and floor of the reverberation chamber and each other to reduce correlation between measurements. The test signals were generated using the loudspeaker, and were then recorded simultaneously using two microphones for 10 seconds. The signals were acquired after at least 10 seconds from the initial signal excitation in order to ensure steady state condition, since a duration of 10 seconds is similar to the representative reverberation time of the room. Each signal was measured for 15 different separation distances $r = |\mathbf{y} - \mathbf{x}|$ using Eq. . The spatial correlation coefficient for each separation distance r was estimated by averaging the measurements at 10 different positions in the reverberation chamber. To summarize, the measurement duration of $T=10$ seconds was used with $\Delta T=1/8192$ and $M=81920$, and the spatial averaging of $N=10$ was used in Eq. for 15 discrete values of r .

4.2 Averaging operation

The calculation of the spatial correlation coefficient is based on time and space averaging operations. The length of time averages was chosen to satisfy the condition that the error due to finite averaging time is much lower than the error due to finite spatial averaging¹⁷. In this experiment, 10 seconds of time duration for broadband signals was sufficient to consider the estimation error of the time integral to be negligible.

The number of spatial averages required to achieve a good estimation of the spatial correlation coefficient should be also considered. If a sufficiently large number of spatial averages are performed, almost any sound field shows the same characteristics as a diffuse sound field¹⁸. In other words, the spatial average operation increases the degree of measured diffuseness when the orientations of the measurement points in space are chosen randomly. In practice, the more diffuse the sound field is, the less spatial averages are required to obtain an accurate estimate.

In particular, the sound field excited by a signal of a low frequency band requires more spatial averages to achieve the same estimation accuracy compared to that excited by the signal of a high frequency band with the same bandwidth. Therefore, the number of spatial averages depends on the frequency band and the requirements for accuracy of the specific application. In this experiment, the number of spatial averages was fixed to ten to compare experimental results with each other under the same conditions.

4.3 Calculation of the spatial correlation coefficients

Figure 3 shows the power spectral density of each test signal measured at one typical position in the reverberation chamber. Curves in Fig. 3 are different from those in Fig. 1. The main reason is that the frequency response of the loudspeaker-microphone pair and the room influenced the measured power spectral density of each signal. This difference was therefore compensated for by substituting the measured power spectral density for $G(f)$ in Eq. . The dashed lines in Fig. 4, 5, and 6 represent the theoretical predictions using the measured power spectral density.

The theoretical predictions of the spatial correlation coefficients for the test signals were calculated from Eq. by substituting the theoretical power spectral densities in Table II for $G(f)$ with a frequency resolution of 0.1Hz and $L=40960$. The solid lines in Fig. 4, 5, and 6 represent these theoretical predictions.

The measured spatial correlation coefficients were calculated from Eq. , and are presented by the circles in Fig. 4, 5, and 6 for the three test signals in Table I . The total length of the error bar at each measured value is twice the standard deviation of the spatial correlation coefficient at the corresponding separation distance $r = |\mathbf{y}_n - \mathbf{x}_n|$.

4.4 Results

Figure 4 shows the spatial correlation coefficients of the test signal whose bandwidth is from 0Hz to 1kHz. This broadband signal includes frequency components below the Schroeder frequency, which are believed to be the main source of discrepancy between measured values and theoretical predictions. In this case, the use of measured power spectral density does not improve the estimation of the spatial correlation coefficients significantly. Therefore the main cause of prediction error is assumed to be imperfect diffuseness at low frequencies. In spite of some discrepancy, theoretical predictions were comparable with experimental results in this case since the sound field in the frequency band above the Schroeder frequency dominates the sound field in the frequency band below it. If the bandwidth of the signal above the Schroeder frequency is broader, the estimation error is expected to be smaller.

Figure 5 shows the spatial correlation coefficients of the test signal whose bandwidth is from 0Hz to 350Hz, which is entirely below the Schroeder frequency. The discrepancy between measured values and theoretical predictions using the theoretical power spectral density (solid line) are much larger than that of the previous case due to the dominant low frequency components. The standard deviation of the estimate is also larger than that of other cases due to the smaller degree of diffuseness. In this case, the use of measured power spectral density improves to some extent the estimation of the spatial correlation coefficients. Therefore the main causes of prediction error are assumed to be both imperfect diffuseness and imperfect estimation of the power spectral density at low frequencies.

Figure 6 shows the spatial correlation coefficients of the test signal whose bandwidth is from 350Hz to 1kHz, which is entirely above the Schroeder frequency. The discrepancy is very small, that is, the measured spatial correlation coefficient agrees well with the theoretical prediction.

As discussed earlier, the theoretical prediction for the broadband spatial correlation coefficients has two main sources of estimation error originating from the sinc function term and the power spectral density term in Eq. . Both errors are significant in the low frequency band, particularly below the Schroeder frequency. However, although a signal includes very low frequency band, if the frequency components above the Schroeder frequency are sufficiently broad, the estimation errors can still be acceptable if they are below some limit that depends on the desired precision required by an application.

Figure 7 shows the measured and theoretical spatial correlation coefficients for a 1kHz pure tone calculated as above, which are presented here for comparison with previous studies. It shows large standard deviation due to the very narrow band of the pure tone, with reasonable discrepancy between theoretically predicted and measured values.

5. CONCLUSION

In this paper, spatial correlation coefficients of broadband sound fields were measured in a reverberation chamber, and experimental results were compared with theoretical predictions. Theoretical predictions showed good agreement with experimental results when the frequency components of the generated signal were entirely above the Schroeder frequency. When a broadband signal entirely below the Schroeder frequency was generated, the estimation error was larger than that of other cases but could be reduced by using the measured power spectral density in the theoretical predictions. In the case of a broadband signal that included frequency bands both below and above the Schroeder frequency, theoretical predictions were comparable with experimental results since the bandwidth of the signal above the Schroeder frequency was sufficiently broad. These results can facilitate the use of broadband acoustic signals in diffuse field measurements and applications.

REFERENCES

- ¹K. Bodlund, "A new quantity for comparative measurements concerning the diffusion of stationary sound fields," *J. Sound Vib.* **44**, 191–207 (1976).
- ²"Acoustics – determination of sound power levels of noise sources – precision methods for broadband sources in reverberation rooms," ISO standard 3741–1988.
- ³D. Lubman, "Spatial averaging in a diffuse sound field," *J. Sound Vib.* **46**, 532–534 (1969).
- ⁴P. A. Nelson and S. J. Elliott, *Active Control of Sound* (Academic, London, 1992).
- ⁵B. Rafaely, "Zones of quiet in a broadband diffuse sound field," *J. Acoust. Soc. Am.* **110**, 296–302 (2001).
- ⁶R. K. Cook, R. V. Waterhouse, R. D. Berendt, S. Edelman, and M. C. Thomson Jr., "Measurements of correlation coefficients in reverberant sound fields," **27**, 1072–1077 (1955).
- ⁷F. Jacobsen, "The diffuse sound field," The Acoustics Laboratory, Technical University of Denmark, Report No. 27 (1979).
- ⁸H. Nélisse and J. Nicolas, "Characterization of a diffuse field in a reverberant room," *J. Acoust. Soc. Am.* **101**, 3517–3524 (1997).
- ⁹B. Rafaely, "Spatial-temporal correlation of a diffuse sound field," *J. Acoust. Soc. Am.* **107**, 3254–3258 (2000).
- ¹⁰T. J. Schultz, "Diffusion in reverberation rooms," *J. Sound Vib.* **16**, 17–28 (1971).

- ¹¹C. L. Morfey, *Dictionary of Acoustics* (Academic, London, 2001).
- ¹²F. Fahy, *Foundations of Engineering Acoustics* (Academic, London, 2001).
- ¹³A. D. Pierce, *Acoustics—An Introduction to Its Physical Principles and Application* (Acoustical Society of America, New York, 1989).
- ¹⁴M. R. Schroeder, "On frequency response curves in rooms. comparison of experimental, theoretical, and Monte Carlo results for the average frequency spacing between maxima," J. Acoust. Soc. Am. **34**, 76–80 (1962).
- ¹⁵D. E. Johnson, *Introduction to Filter Theory* (Prentice Hall, London, 1976)
- ¹⁶I. Chun, "Experimental investigation of spatial correlation of broadband diffuse sound fields," MSc thesis, ISVR, University of Southampton, 2000.
- ¹⁷D. Lubman, "Spatial averaging in sound power measurements," J. Sound Vib. **16**, 43–58 (1971).
- ¹⁸F. Jacobsen and T. Roisin, "The coherence of reverberant sound fields," J. Acoust. Soc. Am. **108**, 204–210 (2000).

TABLES

Table I. Test signals.

Number	Bandwidth	Order of filter	Cut-off frequency of filter
1	0Hz ~ 1000Hz	16 th order lowpass filter	1000Hz
2	0Hz ~ 350Hz	8 th order lowpass filter	350Hz
3	350Hz ~ 1000Hz	4 th order bandpass filter	350Hz and 1000Hz

Table II. One-sided power spectral density of each test signal.

Test signal number	One-sided power spectral density
1	$2 \times \frac{1000^{32}}{f^{32} + 1000^{32}} \times S_w$
2	$2 \times \frac{350^{16}}{f^{16} + 350^{16}} \times S_w$
3	$2 \times \frac{f^8 \cdot (1000 - 350)^8}{f^8 \cdot (1000 - 350)^8 + (1000 \times 350 - f^2)^8} \times S_w$

FIGURE CAPTIONS

Figure 1 Theoretical power spectral density of each test signal with bandwidth:

(a) 0Hz~1kHz (b) 0Hz~350Hz (c) 350Hz~1kHz.

Figure 2 Block diagram of the measurement system.

Figure 3 Power spectral density of the each test signal measured in the reverberation Chamber with bandwidth: (a) 0Hz~1kHz (b) 0Hz~350Hz (c) 350Hz~1kHz.

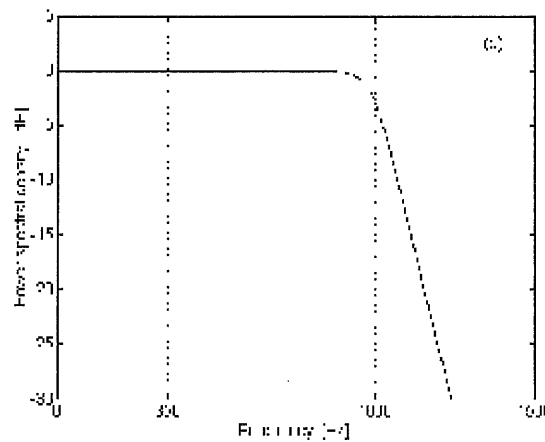
Figure 4 Spatial correlation coefficient of the test signal with bandwidth of 0Hz~1kHz (circles: measured values, error bar : standard deviation of the estimate, solid line : theoretical predictions using the theoretical power spectral density, dashed line : theoretical predictions using the measured power spectral density).

Figure 5 Same as Figure 4, except bandwidth : 0Hz~350Hz.

Figure 6 Same as Figure 4, except bandwidth : 350Hz~1kHz.

Figure 7 Spatial correlation coefficient of 1kHz sinewave (circles: measured values, error bar : standard deviation of the estimate, solid line : theoretical predictions).

FIGURES



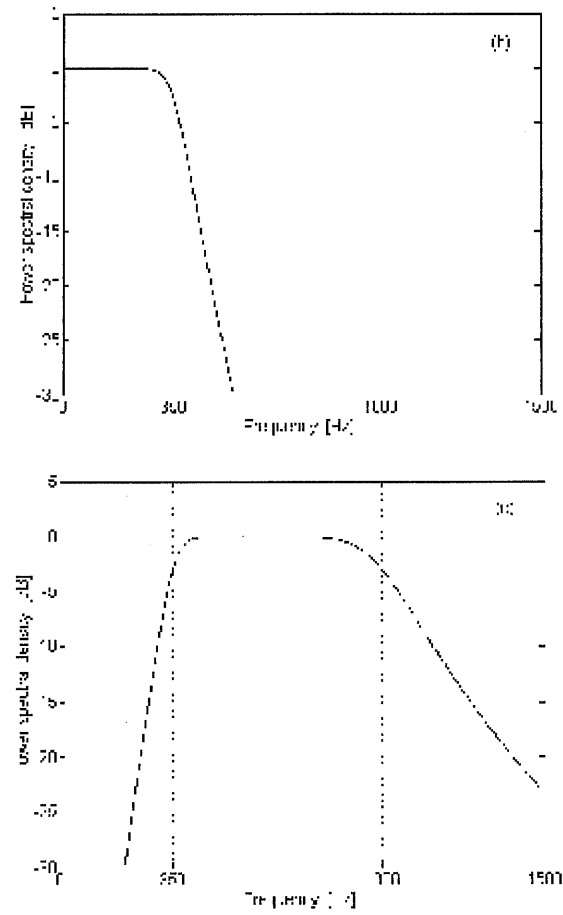


Figure 1.

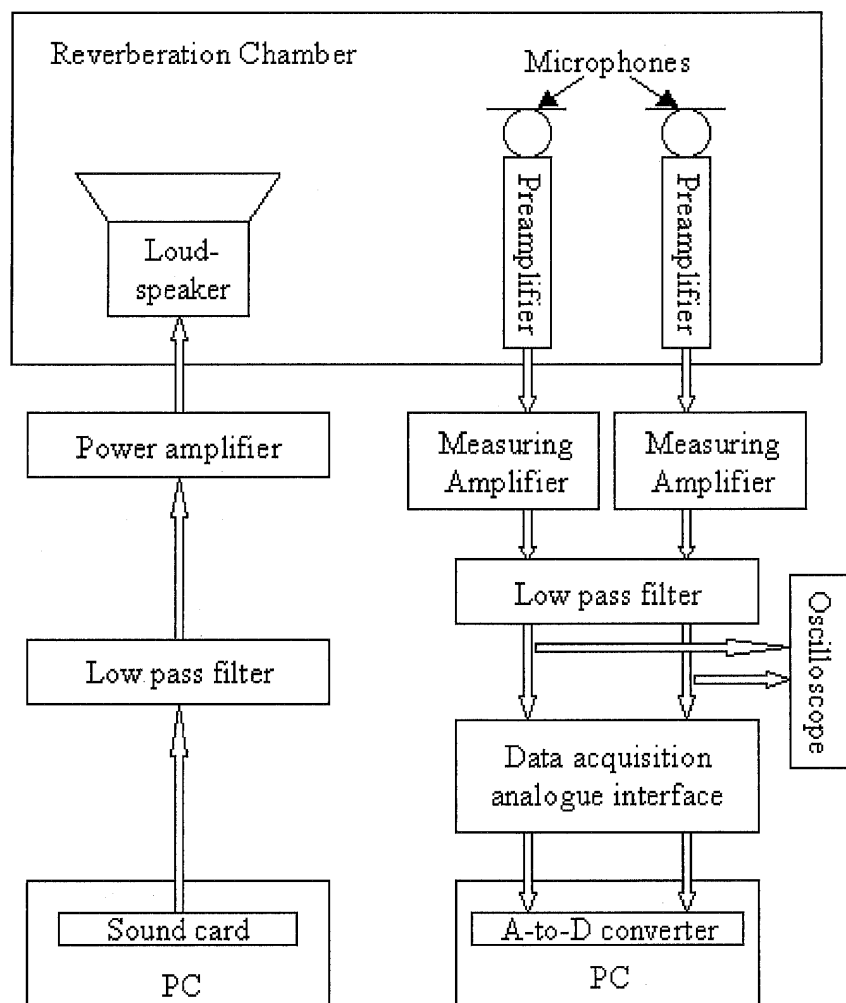


Figure 2.

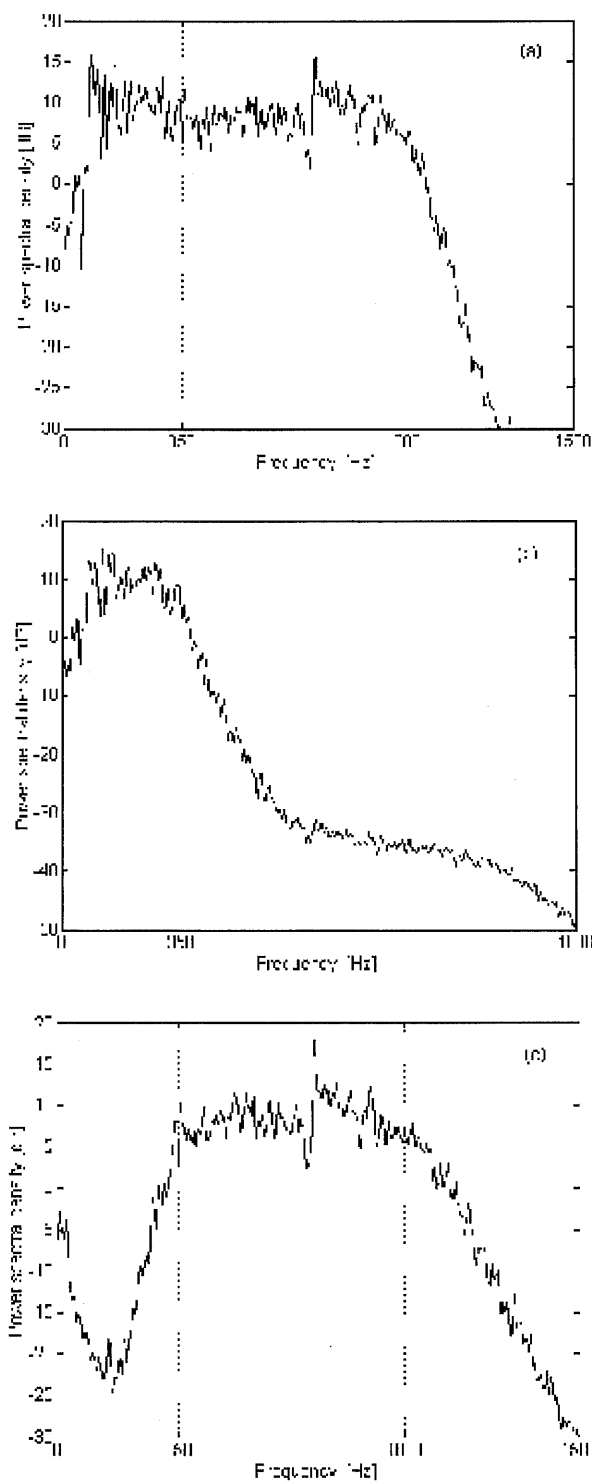


Figure 3.

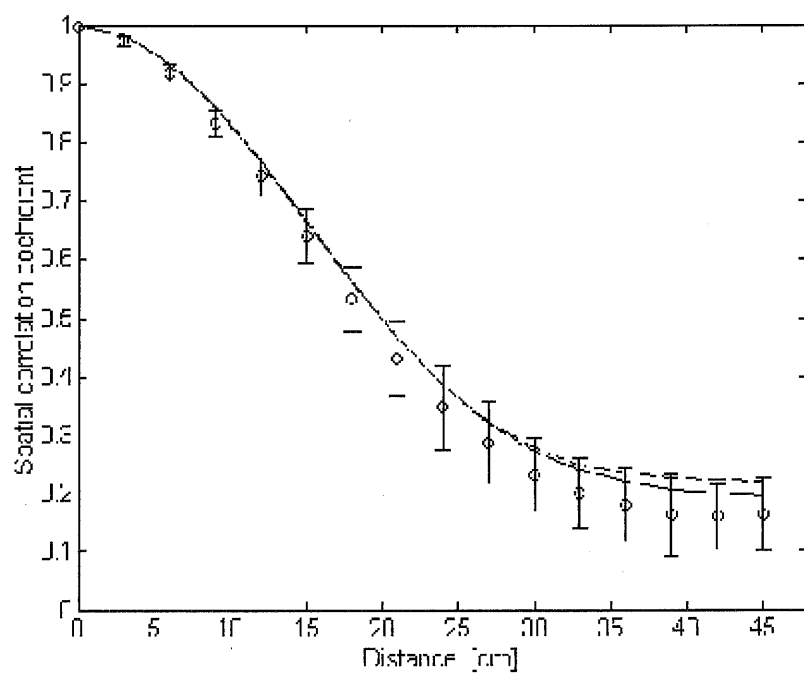


Figure 4.

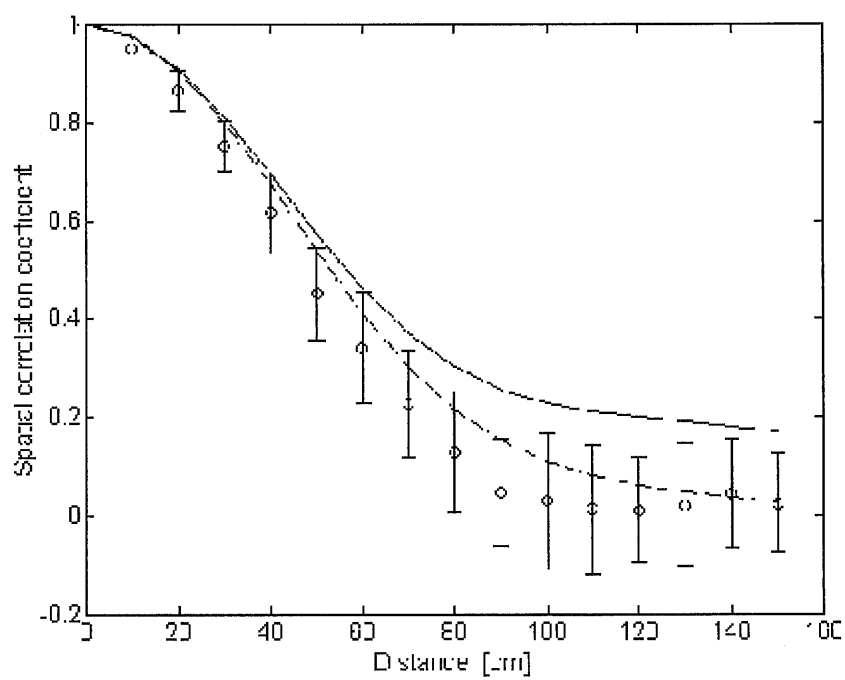


Figure 5.

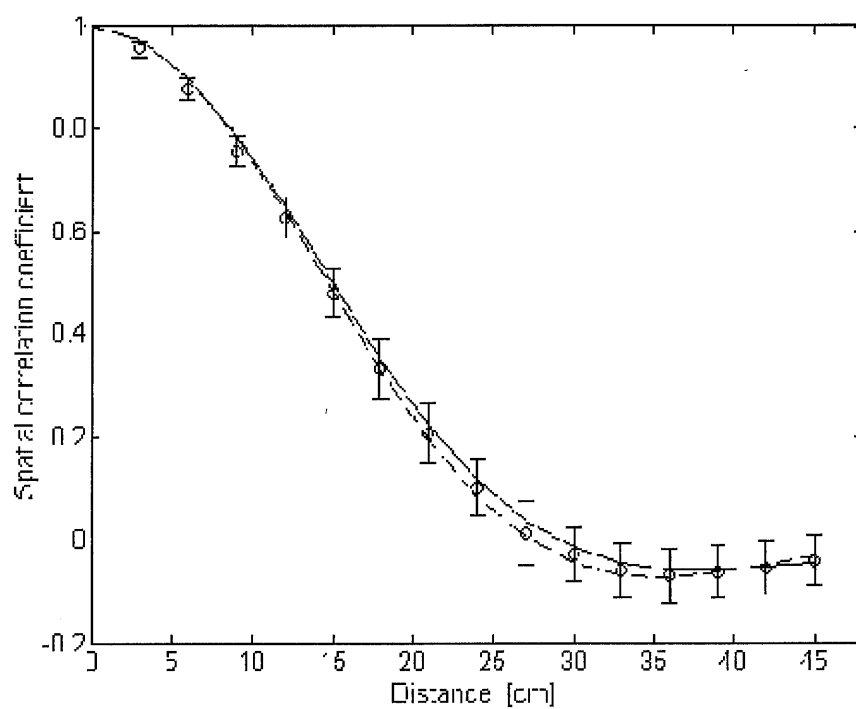


Figure 6.

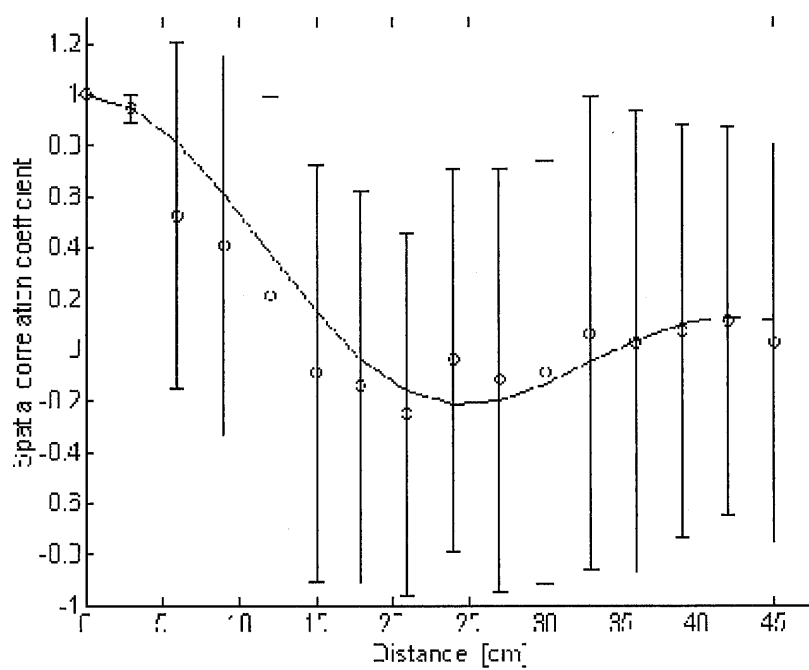


Figure 7.